Nonradiative energy transfer without lifetime quenching in doped Mn-based crystals

B. Di Bartolo*
Department of Chemistry, Massachusetts Institute of Technology, Cambridge, Massachusetts 02139

J. Danko† and D. Pacheco‡
Department of Physics, Boston College, Chestnut Hill, Massachusetts 02167
(Received 19 August 1986)

It is generally considered that the introduction of acceptors into a crystal will result in a lowering of the luminescence output and lifetime of the host ions (the donors). In rare-earth-doped, Mn-based crystals, this is not the case. Although the luminescence output of the host Mn ions is significantly affected by the presence of the rare-earth ions, the luminescence lifetime of the Mn emission is relatively unaffected. In this study the systems investigated include MnF_2, $RbMnF_3$, $RbMn_{0.8}Mg_{0.2}F_3$, $RbMn_{0.4}Mg_{0.6}F_3$, $RbMnF_3$:Nd^{3+}, and MnF_2:Er^{3+}. Luminescence spectra, excitation spectra, and lifetime measurements over the 4—300-K range are presented to demonstrate the above behavior. A physical model is developed to explain the observed features, including the lack of quenching of the luminescence lifetime of the Mn ions. The analysis includes quantitative estimates of the activation energy for the quenching of Mn emission and the coupling strength between perturbed and unperturbed Mn ions.

I. INTRODUCTION

Nonradiative energy transfer between donor and acceptor ions in solids takes place through various processes, e.g., dipole-dipole or exchange. Migration of excitation energy among donors may occur before this transfer, and this influences the time evolution of the donor and acceptor luminescence. Three regimes are generally considered:[1] (i) energy transfer with no migration among donors, for small donor concentrations, (ii) diffusion-limited energy transfer from donor to acceptors, for larger donor concentrations, and (iii) fast diffusion among donors for very large donor concentrations. For the first two cases, the donor luminescence decay is nonexponential; in principle it can provide information on the nature of the donor-acceptor energy-transfer process. For the third case, the donor luminescence decay is purely exponential. In all three regimes, the transfer rate is dependent on the concentration of the acceptors. The point to be made here is that, regardless of the process present, the decay pattern of the donor ions should be affected by the presence of the acceptor ions.

Stoichiometric Mn-based crystals, such as MnF_2 and $RbMnF_3$, doped with rare-earth ions present an interesting exception to this rule. The luminescence of the undoped samples is associated mostly with localized, impurity-induced Mn traps[2] which are present in concentrations on the order of only ten parts per million. Energy transfer among unperturbed Mn^{2+} ions assures the prompt excitation of these traps and their efficient emission. When these systems are doped with rare-earth ions (REI's), Mn→REI energy transfer is often observed. In such systems the decay pattern of the donor (Mn) luminescence is *not* affected by the presence of the REI.

The purpose of this investigation is to elucidate the reasons for this phenomenon by comparing the spectra characteristics of stoichiometric and nonstoichiometric Mn-based systems, such as $RbMnF_3$ and $RbMn_xMg_{1-x}F_3$ with those of Mn-based systems doped with rare-earth ions (specifically, $RbMnF_3$:Nd^{3+} and MnF_2:Er^{3+}.)

Being stoichiometric, $RbMnF_3$ exhibits some luminescence which is due to emission from the decay of nonlocalized excitations. This "intrinsic" Mn luminescence includes (1) the so-called exciton lines which represent the purely electronic deexcitation of the crystal, (2) magnon-assisted lines, which represent the electronic deexcitation of the crystal, accompanied by spin-wave (magnon) excitation, and (3) the phonon sidebands to these lines. This sharp-line intrinsic structure, however, is dwarfed by the long-lived emission from impurity-induced, localized Mn luminescence centers. In fact, in order to study the intrinsic luminescence, it is necessary to have sample temperatures below 10 K and preferably use time-resolved spectroscopy techniques.[3]

Mn^{2+} ions in the vicinity of certain impurities, present in concentrations of only ten parts per million, emit the dominant sharp-line luminescence of stoichiometric Mn-based crystals. In MnF_2, the intense sharp-line Mn emission in the spectral range 5450—5550 Å has been specifically attributed to the presence of Ca^{2+}, Zn^{2+}, and Mg^{2+} impurities.[2] The result of this perturbation is a lowering of the Mn^{2+} ion's excited energy levels. The strong luminescence from this perturbed center is indicative of an efficient transfer of excitation among the relatively unperturbed Mn^{2+} ions. At sufficiently low temperatures, the perturbed Mn^{2+} ions trap the excitation and emit the resultant luminescence; this emission may be referred to as "extrinsic" Mn luminescence. It is this luminescence that will be considered here.

II. EXPERIMENTAL TECHNIQUES

The absorption spectra described below were obtained by means of a Cary model no. 14R spectrophotometer.

The luminescence spectra were obtained by exciting the sample, mounted in a Janis 8DT cryostat, with the light from a GE Quartzline DVY 650-W source, filtered through a $CuSO_4$ solution (3500—5300-Å bandpass). The luminescence was observed at 90° to the direction of excitation, chopped and focused onto the entrance slit of a McPherson model no. 2051 scanning monochromator (blazed at 1.25 μm), which has a dispersion of 15 Å/mm. When observing the luminescence in the optical region the signal was detected by either a RCA 7102 (S-1) or a 7265 (S-20) photomultiplier, amplified by a PAR model no. 122 phase-sensitive detector, and displayed on a strip-chart recorder. The 7102 photomultiplier was cooled by crushed dry ice. When observing the luminescence in the infrared region, a lead sulfide detector with a builtin preamplifier replaced the photomultiplier.

The excitation measurements were performed by selectively pumping the sample under consideration with the Quartzline source in conjunction with a Jarrell-Ash model no. 82-410 scanning monochromator (blazed at 0.6 μm) and then detecting the output by means of proper interference filters. For the excitation spectra, the RCA 7102 photomultiplier was employed.

The pulsed-luminescence measurements were made by exciting the sample with EG&G FX-12 or FX-33 flashtubes. The emission was monitored by use of appropriate interference filters in conjunction with the RCA 7102 or 7265 photomultipliers or a lead sulfide detector and then photographed on a Tektronix oscilloscope. Measurements were also made using a Molectron model no. UV12 nitrogen laser-pumped DL14 dye laser. The signal was detected by the RCA 7265 photomultiplier via the McPherson monochromator which was set at the appropriate wavelength. The electrical signal was directed to a PAR model no. 164 gated integrator connected to a PAR model no. 162 boxcar averager.

The temperature of the samples was varied by means of an exchange-gas technique.

III. SPECTRAL CHARACTERISTICS OF NOMINALLY PURE Mn-BASED CRYSTALS

The specific data presented here pertain to $RbMnF_3$.[4,5] The energy-level scheme of Mn^{2+} and the absorption spectrum of $RbMnF_3$ at 78 K appear in Figs. 1 and 2, respectively. The bands are labeled according to the notation used by Mehra and Venkateswarlu[6] in their studies of this crystal. The bands correspond to transitions from the ground state to the excited levels indicated in Table I. Sharp-line absorption features appear when the temperature approaches 4 K.

As for the emission we observed the following.

(1) The highly temperature-dependent emission of $RbMnF_3$ (see Fig. 3) consists of two broad bands that peak at ~5700 and ~6400 Å, and a number of sharp lines. These lines represent electronic and magnon-assisted transitions of impurity-induced localized Mn^{2+} luminescence centers;[5] the broad bands are thought to be multiphonon sidebands of such lines. With reference to Fig. 3 we note that after a slight increase in the intensity from 9 to 11 K, the higher-energy emission band de-

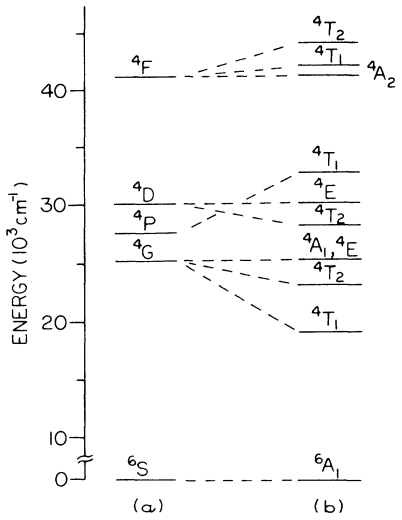

FIG. 1. Energy-level scheme of (a) the free Mn^{2+} ion and (b) Mn^{2+} in the crystal field of $RbMnF_3$.

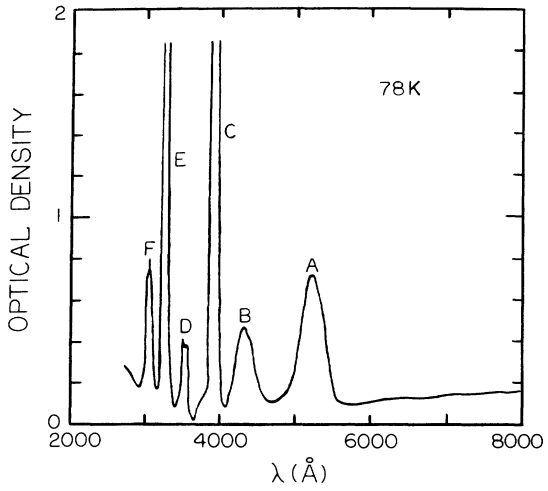

FIG. 2. Absorption spectrum of $RbMnF_3$ at 78 K.

TABLE I. Transitions of Mn as represented in the absorption spectrum of $RbMnF_3$.

Absorption peaks	Transitions $^6A_1(S)\rightarrow$
A	$^4T_1(G)$
B	$^4T_2(G)$
C	$^4E(G)$, $^4A_1(G)$
D	$^4T_2(D)$
E	$^4E(D)$
F	$^4T_1(P)$

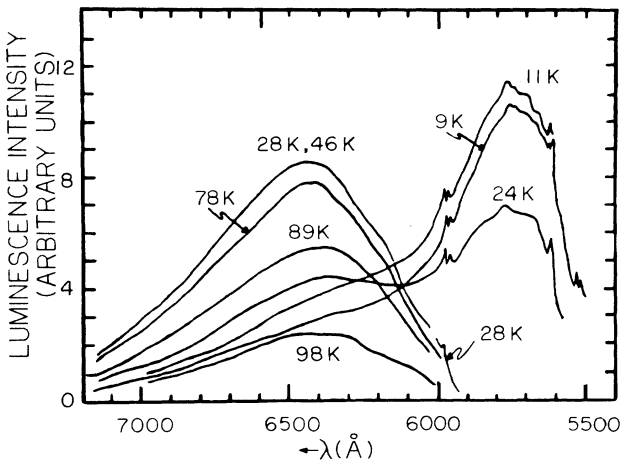

FIG. 3. Thermal dependence of the luminescence spectrum of $RbMnF_3$.

creases rapidly with increasing temperature. This thermal quenching is accompanied by the temperature enhancement of the lower-energy emission band. In fact, by 28 K, it is only the lower-energy band that remains, and at that point, this band's intensity is comparable to that once achieved by the higher-energy band at low temperature. Such enhancement of the lower-emission band has been detected in other stoichiometric Mn-based crystals, including $KMnF_3$ and $BaMnF_4$.[7] The lower-energy emission band eventually decreases with further rise in temperature, in accord with its lifetime dependence on temperature, and becomes very weak beyond 120 K.

(2) Excitation measurements of the emissions from the two bands correlate very well with the absorption spectra; this indicates that all the Mn^{2+} ions are excited via the same absorption bands.

(3) The pulsed luminescence measurements, reported in Fig. 4, reflect the fact that each band may be generally associated with a single lifetime at all temperature; however in the temperature regions 7—11 and 25—30 K a luminescence *rise* precedes an otherwise purely exponential decay for the lower-energy band. We note that the region 25—30 K is the one at which the higher-energy band quenches; therefore the rise of the luminescence signal in this region is a possible indication of the feeding of the lower band by the upper band. The luminescence rise in the other region, 7—11 K may be due to the emptying into the A level of some shallower trap.

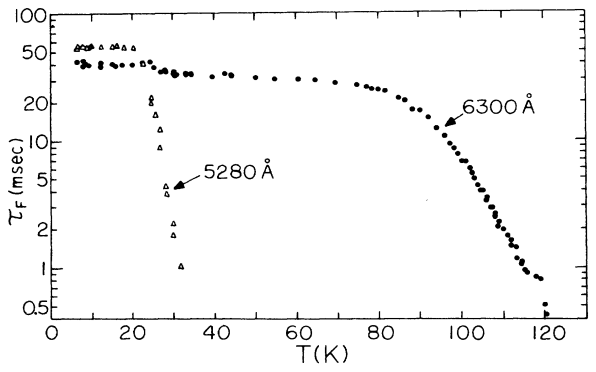

FIG. 4. Thermal dependence of the lifetime of the two broad emission bands of $RbMnF_3$.

IV. SPECTRAL CHARACTERISTICS OF NONSTOICHIOMETRIC Mn-BASED CRYSTALS

The specific data of this section pertain to $RbMn_xMg_{1-x}F_3$ with $x=0.8$ and 0.4.[8] Figures 5 and 6 show the thermal dependence of the luminescence spectra for these two crystals. Once again, using lifetime measurements (see Figs. 7 and 8) one is able to detect the presence of two distinct temperature-dependent emission bands; the more energetic band thermally quenches at low temperature, followed by the quenching of the remaining band by ~ 120 K. As with $RbMnF_3$, excitation measurements indicate that both bands are activated via the absorption bands of Mn^{+2}. The lower-energy band, seen as a "shoulder" to the higher-energy emission by Koumvakalis *et al.*[9] in their studies of $RbMn_{0.7}Mg_{0.3}F_3$ and $RbMn_{0.4}Mg_{0.6}F_3$, is, in fact, a second distinct emission band.

In contrast to the fully concentrated system $RbMnF_3$, the following features of $RbMn_{0.8}Mg_{0.2}F_3$ and $RbMn_{0.4}Mg_{0.6}F_3$ are noted.

(1) No sharp-line structure is present.

(2) The peak positions of the two emission bands are shifted toward longer wavelengths (5750→6000 Å and 6440→6500 Å).

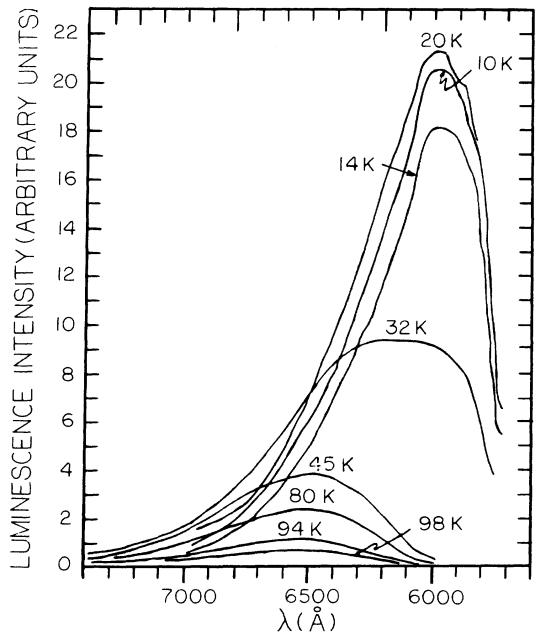

FIG. 5. Thermal dependence of the luminescence spectrum of $RbMn_{0.8}Mg_{0.2}F_3$.

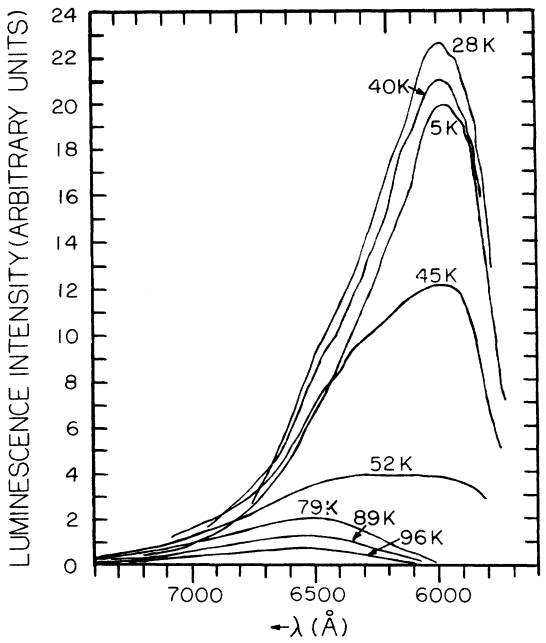

FIG. 6. Thermal dependence of the luminescence spectrum of $RbMn_{0.4}Mg_{0.6}F_3$.

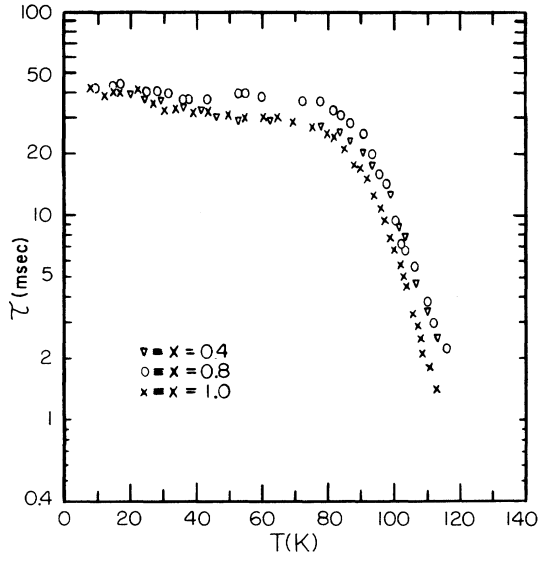

FIG. 8. Thermal dependence of the lifetime of the lower-energy emission band of $RbMn_xMg_{1-x}F_3$.

(3) A luminescence rise is no longer detectable. Both bands exhibit single decays throughout the temperature range studied.

(4) The higher-energy emission has a slower falloff with increasing temperature and is thermally quenched at a higher temperature; the lower the Mn concentration, the higher the quenching temperature.

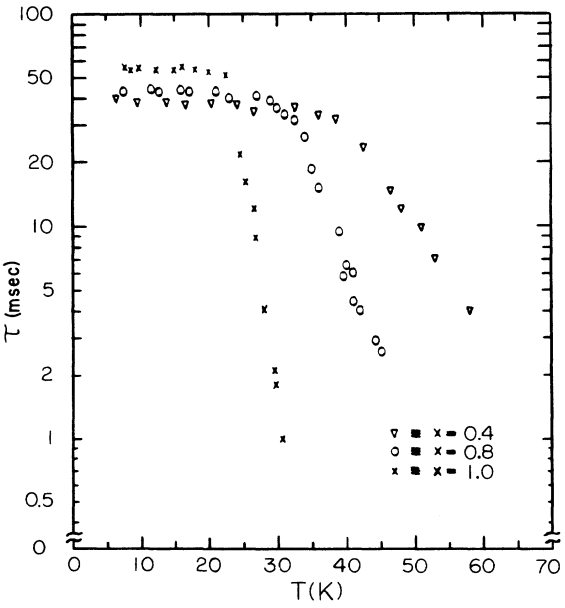

FIG. 7. Thermal dependence of the lifetime of the upper-energy emission band of $RbMn_xMg_{1-x}F_3$.

(5) The high-energy band exhibits a shorter lifetime at low temperature; the lower the Mn concentration, the shorter the lifetime.

(6) The thermal dependence of the lifetime of the lower-energy emission band is essentially unaffected.

(7) The enhancement of the lower-energy band does not accompany the quenching of the higher-energy emission nor does the peak intensity of this lower-energy band ever reach more than a fraction of that achieved by the higher-energy emission at low temperature.

The lack of sharp-line emission in the two nonstoichiometric Mn crystals is not surprising. First of all, due to the significant increase in the average spacing between Mn ions in the latter crystals over that in $RbMnF_3$, it is expected that the probability of a magnon-assisted transition is substantially reduced. This would be reflected in a reduction of the intensity of all magnon sidebands, including the extrinsic 1-magnon sidebands which dominate the observed sharp-line structure in $RbMnF_3$. Second, the increased Mg concentration is expected to result in an inhomogeneous broadening of the sharp emission lines. In fact, based on the work of Hegarty *et al.*[10] on $MnF_2:Zn^{2+}$, the strain due to such a high concentration of Mg^{2+} ions in the two nonstoichiometric crystals should be sufficient to broaden all remaining sharp lines beyond the level of detection.

The bulk of the luminescence of $RbMnF_3$ is attributed to Mn emission from two distinct, localized traps; the broad emission bands represent multiphonon sidebands of the transitions from the trap levels to the ground state. It is reasonable to assume the same nature for these bands in the nonstoichiometric crystals. The effect of a decreasing Mn^{2+} concentration on the peak position of the two broad emission bands is probably due in part to their complex composition.

V. Mn-Mn ENERGY TRANSFER

The lifetime of the higher-energy band in $RbMn_xMg_{1-x}F_3$ for $x=1.0$, 0.8, and 0.4 was found to exhibit a thermal dependence of the type

$$\tau^{-1}=p_0+p_1e^{-\Delta E/kT}. \quad (1)$$

The fitting of the experimental data with this formula for $RbMnF_3$ is shown in Fig. 9. The parameters obtained by performing the fittings for all crystals are reported in Table II.

As for the physical meaning of the two terms in (1), p_0 represents the inverse of the lifetime at very low temperature and the second term indicates the presence of an activation process. Since the difference in energy ΔE corresponds approximately to the separation in energy between the upper edge of the emission band and the lower edge of the absorption A band, the above dependence indicates that the higher-energy emission band quenches by thermal activation to the A level of the relatively unperturbed Mn^{2+} ions.

The fact that localized Mn traps, present in $RbMnF_3$ at a concentration on the order of only ten parts per million, are responsible for nearly all of the luminescence of the crystal is direct evidence of the existence of an efficient transfer of excitation among the relatively unperturbed Mn^{2+} ions in the stoichiometric crystal. In the model that we discuss in Sec. VIII of this paper, we interpret p_1 as being the lower limit value for the probability per unit time of energy transfer between two nearest-neighbor Mn^{2+} ions. We note at this point that the behavior of p_1 as a function of concentration is thus indicative of the expected decrease in transfer rate with decreasing Mn concentration.

The temperature dependence of the lifetime of the lower-energy band cannot be reasonably fitted with a formula like (1). In addition, the curves for the three Mn^{2+} concentrations are nearly identical. The quenching of the lower-energy emission band of $RbMn_xMg_{1-x}F_3$ is, therefore, not by thermal activation to the A level, but is probably by a multiphonon decay to the ground level. The Mn^{2+} concentration would thus affect only the feeding of this deeper trap, not the quenching of its emission.

TABLE II. Fitting parameters for the lifetime of the $RbMn_xMg_{1-x}F_3$ higher-energy emission band.

Mn^{2+} (at. %)	ΔE (cm^{-1})	p_0 (sec^{-1})	p_1 (sec^{-1})
100	300±5	18.2±0.3	$(1.0\pm0.25)\times10^9$
80	294±7	23.3±0.5	$(5.0\pm1.0)\times10^6$
40	265±6	26.3±0.8	$(1.5\pm0.2)\times10^5$

The reduced indirect transfer of excitation between the two Mn luminescence traps in the nonstoichiometric samples (via the less-perturbed Mn^{2+} ions) is best indicated in Fig. 10, (where τ_1 and τ_2 represent the lifetimes of the high-energy and of the low-energy emission bands, respectively). This figure depicts the total integrated luminescence intensity (in number of photons emitted) for each of the three crystals at temperatures up to 110 K. (The total integrated luminescence intensity is equal to the area under the luminescence intensity versus λ curve. The curve first is corrected for instrumental spectral sensitivities and by the factor λ.) Normalization of the integrated intensity data of each sample was such as to clearly indi-

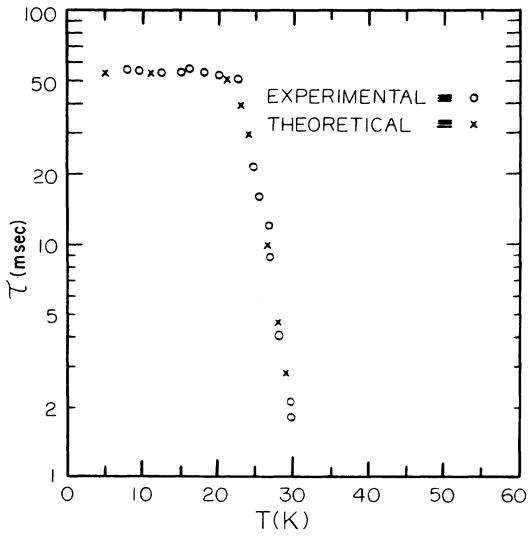

FIG. 9. Theoretical fitting of the temperature-dependent lifetime of the upper-energy emission band of $RbMnF_3$.

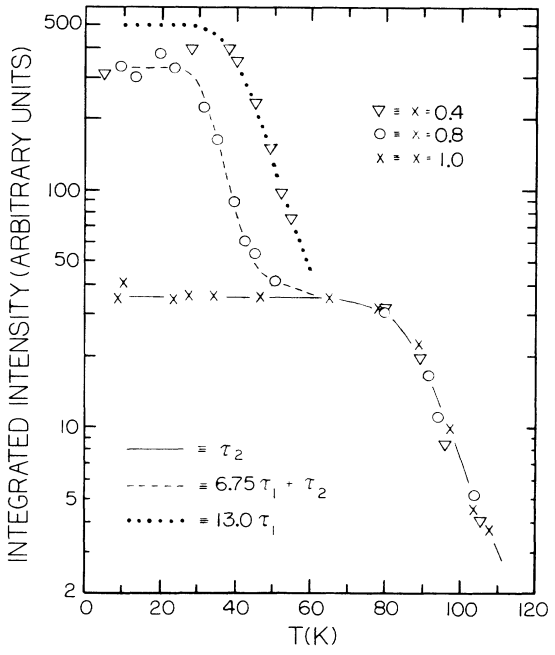

FIG. 10. Thermal dependence of the total integrated luminescence intensity of $RbMn_xMg_{1-x}F_3$ (corrected for the instrumental spectral sensitivities).

cate the same thermal dependence beyond ~ 70 K, as that of τ_2, the lifetime of the lower-energy emission band. This dependence is not surprising since it is only the lower-energy band that emits in these crystals in this temperature range. The result of this normalization is that the total integrated luminescence intensity of $RbMnF_3$ exhibits a thermal behavior like τ_2; $RbMn_{0.8}Mg_{0.2}F_3$ like $(6.75\tau_1+\tau_2)$; and $RbMn_{0.4}Mg_{0.6}F_3$ like $(13\tau_1+\tau_2)$.

It is apparent from Fig. 10 that the integrated intensity of the 100-at.% Mn sample remains relatively constant well beyond the quenching temperature of its higher-energy luminescence band. This indicates that the deeper luminescence trap gains all the energy that is thermally activated from the shallower luminescence trap. Trap-to-trap nonradiative transfer, via the less-perturbed Mn ions, is thus very efficient. Since thermal quenching of the lower-energy band is by a downward multiphonon decay, then it would appear that the quenching traps of $RbMnF_3$ play an insignificant role in robbing the crystal of potential luminescence output.

The lack of constancy in the total integrated intensity of the nonstoichiometric crystals, once the higher-energy band starts to quench, is indicative of the fact that the energy which is thermally activated from the shallower luminescence trap simply does not make it to the deeper luminescence trap. Temperature enhancement of the intensity of the lower-energy band is not observed in these crystals. Therefore, the total integrated intensity falls off with increasing temperature much like that of the higher-energy band. Although the transfer among Mn ions, down to a Mn concentration of 40 at.%, is efficient, as previously concluded, it must be that an increased number of quenching sites are introduced during the growth process of the nonstoichiometric crystals which rob the crystal of potential luminescence output in this temperature range.

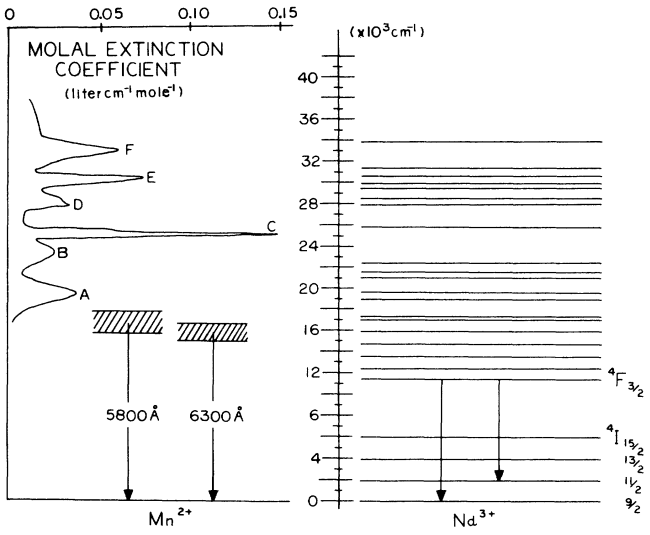

FIG. 11. Energy-level scheme of Mn^{2+} and Nd^{3+} in $RbMnF_3$.

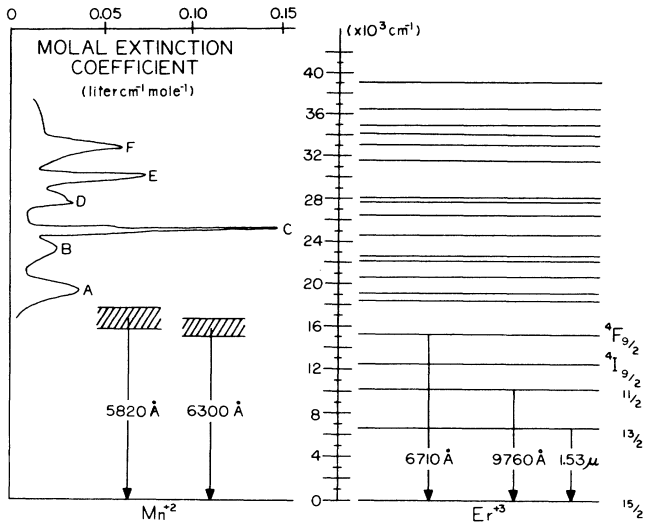

FIG. 12. Energy-level scheme of Mn^{2+} and Er^{3+} in MnF_2.

VI. SPECTRAL CHARACTERISTICS OF RARE-EARTH-DOPED Mn SYSTEMS

We now consider emission in rare-earth-doped Mn systems such as $RbMnF_3$:Nd^{3+} and MnF_2:Er^{3+}. The relevant energy-level schemes are reported in Figs. 11 and 12.

The luminescence spectra of $RbMnF_3$:Nd consist of the Nd^{3+} emission, appearing as two groups of sharp lines centered at 10 500 and 8900 Å and of the broad manganese emission. The variations of the position and intensity of the manganese emission are reported in more detail in Fig. 13. Unlike the Mn emission, the Nd luminescence is still present at and above room temperature.

The luminescence spectra of MnF_2:Er are comprised of

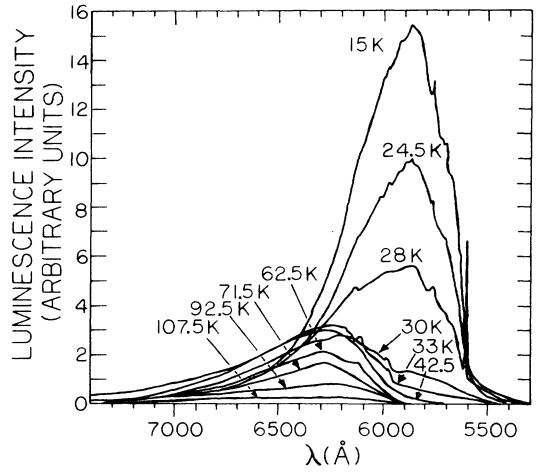

FIG. 13. Thermal dependence of the Mn^{2+} emission in $RbMnF_3$:Nd.

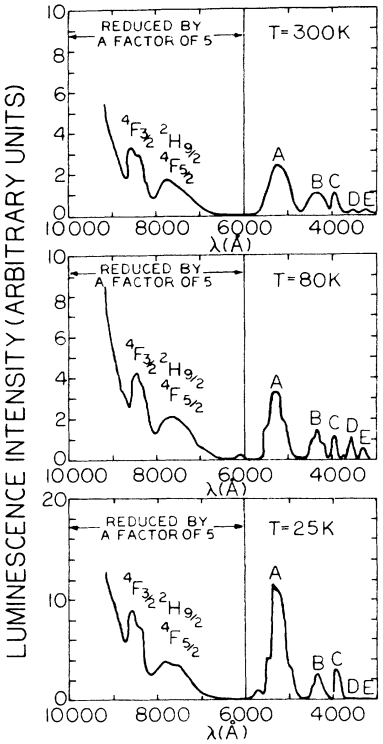

FIG. 14. Excitation spectra of Nd^{3+} in $RbMnF_3$:Nd.

the Er^{3+} emission and the usual Mn emission. The Er^{3+} spectrum consists of three groups of lines centered at 6710 Å, 9700 Å and 1.53 μm, which we assign to transitions from the $^4F_{9/2}$, $^4I_{11/2}$, and $^4I_{13/2}$ levels to the $^4I_{15/2}$ ground level, respectively. As for the Nd case, the Er emission is present at and above room temperature.

VII. Mn→RARE-EARTH ENERGY TRANSFER

The experimental data relating to the transfer of energy from Mn ions to rare-earth to (RE) dopants may be summarized as follows.

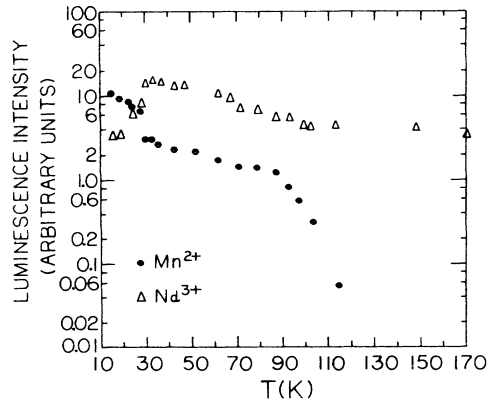

FIG. 15. Thermal dependence of the total integrated luminescence intensities of the Mn^{2+} and Nd^{3+} in $RbMnF_3$:Nd (scales for the Mn^{2+} and Nd^{3+} luminescence are unrelated).

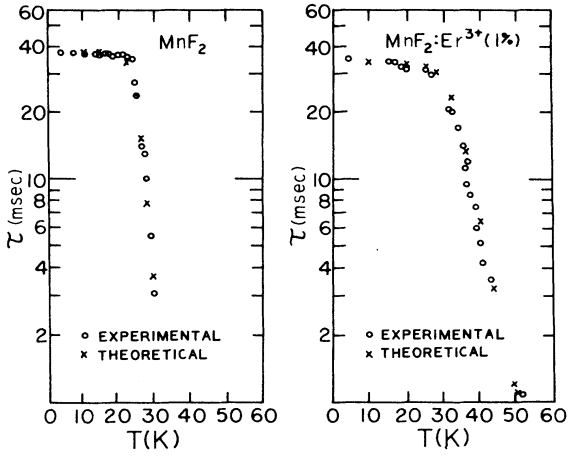

FIG. 16. Thermal dependence of the Mn^{2+} lifetime in MnF_2 and MnF_2:Er at $\lambda = 5820$ Å (Ref. 11).

(1) The excitation spectra of the Nd^{3+} luminescence in $RbMnF_3$:Nd and of the Er^{3+} luminescence in MnF_2:Er reveal the presence of the Mn^{2+} absorption bands. Figure 14 shows the data for Nd^{3+}. These excitation measurements indicate that energy transfer from Mn^{2+} to the RE ions takes place even at room temperature where no Mn^{2+} luminescence is observed. We notice also that the excitation spectra show very little evidence of the presence of rare-earth bands in the optical region where Mn absorbs.

(2) The position and the width of the Mn^{2+} in $RbMnF_3$:Nd are such that this emission overlaps with a Nd^{3+} absorption band ($^4I_{9/2} \rightarrow {}^2G_{7/2}, {}^4G_{5/2}$) below ~ 32 K. Above ~ 32 K the location of the Mn^{2+} emission band does not permit any relevant overlap. Therefore the thermal variation of the total integrated Nd^{3+} luminescence shown in Fig. 15 is opposite to that expected on the basis of the change in the overlap of the observed manganese emission and the neodymium absorption. This would imply that the $Mn^{2+} \rightarrow$REI energy transfer mechanism must be of a nonradiative type.

(3) The total luminescence intensity of Nd^{3+} in $RbMnF_3$:Nd shown in Fig. 15 indicates that the energy transfer increases dramatically in the temperature region where the higher-energy Mn band quenches. Similar behavior is presented by the luminescence of Er^{3+} in MnF_2:Er.

(4) The experimental data points of the Mn^{2+} lifetime in the $RbMnF_3$:Nd sample essentially agree with the corresponding data points of $RbMnF_3$ (Fig. 4), except that below 28 K the lifetimes at 5820 and 6730 Å are *longer*

TABLE III. Fitting parameters for the lifetime of the higher-energy Mn emission in $RbMnF_3$:Nd^{3+}, MnF_2, and MnF_2:Er^{3+}.

	ΔE (cm^{-1})	p_0 (sec^{-1})	p_1 (sec^{-1})
$RbMnF_3$:Nd	300	16.1	6×10^8
MnF_2	250	26.3	4×10^7
MnF_2:Er	250	29.4	10^6

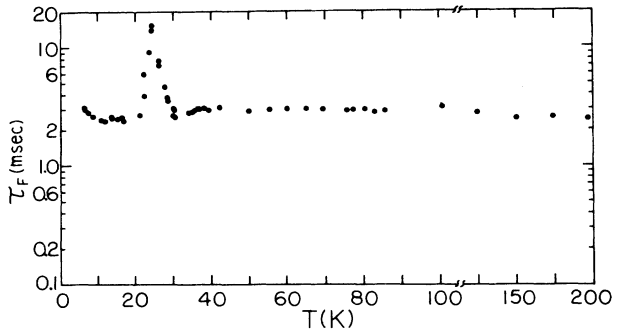

FIG. 17. Thermal dependence of the Nd^{3+} lifetime in $RbMnF_3$:Nd.

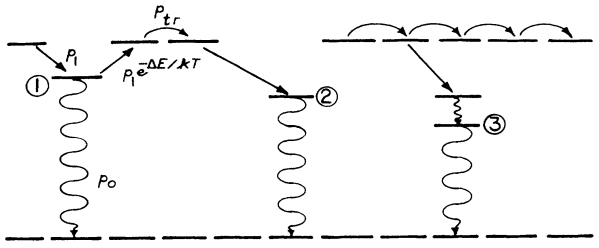

FIG. 18. Deexcitation model.

than those in the undoped sample by ~ 10 to 20 msec and the lower-energy band does *not* present an initial rise in the luminescence signal in the 7–11 K region. The thermal dependence of the lifetime of the higher-energy Mn emission band was fitted to Eq. (1) and the fitting parameters appear in Table III.

(5) Figure 16 reports the lifetime of the higher-energy band for both the pure MnF_2 and MnF_2:Er samples. The theoretical fitting of the lifetime data is included, with the fitting parameters appearing in Table III. As with the pure and RE-doped $RbMnF_3$ crystals, the results are similar for the two samples.

(6) The total integrated emission of the Mn^{2+} emission, however, is strongly affected by the presence of the rare-earth dopants. Contrary to what happens in nominally pure samples the total intensity of the Mn^{2+} emission in the rare-earth-doped samples does not remain constant up to the quenching temperature for the lower-energy Mn emission band, but decreases at the quenching temperature for the higher-energy band. (See for example, Fig. 15.) Correspondingly, the Nd (see Fig. 15) and Er integrated luminescence intensities increase at this temperature.

(7) The $RbMnF_3$:Nd case is of particular interest in that the *intrinsic* Nd lifetime is independent of temperature over the range studied. Any change in the Nd luminescence intensity is due to a change in the energy transferred from Mn to Nd. The characteristics of the resulting Nd^{3+} decay pattern are reported in Fig. 17. In the temperature region between 26 and 38 K, the Nd^{3+} luminescence presents an initial rise followed by a complicated decay with time constants up to ~ 15 msec. The time at which the Nd^{3+} luminescence signal reaches its maximum value, is approximately zero up to ~ 26 K, increases to 1.7 msec at ~ 28 K, and then decreases to zero at ~ 38 K. The decay time of the Nd^{+3} emission is ~ 3 msec outside these temperature regions. The deviation of the Nd^{3+} decay from a pure exponential, which is seen over the same temperature regions in which the higher-energy Mn^{2+} emission band dramatically reduces its intensity, is due to the $Mn^{2+} \rightarrow Nd^{3+}$ energy-transfer process.

VIII. DISCUSSION OF RESULTS

On the basis of these observations we can build up a model that we report in Fig. 18 which provides a physical interpretation of Eq. (1). Three types of localized traps labeled $i = 1,2,3$ are present. Above the trap levels is the first excited energy level of the unperturbed Mn^{2+} ions, i.e., absorption level "*A*". Traps 1 and 2 are responsible for the Mn higher- and lower-energy luminescence bands, respectively. Trap 3 is due to the rare-earth ion. Level *A* is the communication channel between the donor Mn traps and the RE acceptors. That is, such an absorption level preserves its delocalized excitonlike character. Energy is not transferred directly from the Mn traps to the acceptors. Only the energy residing in the shallow Mn trap becomes available for ultimate transfer to the deeper Mn trap or the RE ion.

The low-temperature lifetime of trap 1, essentially radiative, is denoted by p_0^{-1}. The energy-transfer probability per unit time from an unperturbed Mn^{2+} ion to a nearby perturbed Mn^{2+} ion represented by trap 1 is given by p_1 while the probability per unit time of the reverse transfer is given by $p_1 e^{-\Delta E/KT}$. The energy transfer probability per unit time between two nearest-neighbor unperturbed Mn^{2+} ions is denoted by p_{tr}.

It is assumed that $p_{tr} \gg p_1$, so that the p_1 value obtained from the measurements represents a lower limit for p_{tr}. It is due to this condition that the presence of additional traps like 2 or 3 does not affect the lifetime of trap 1. Once the excitation has activated from this trap to a nearby unperturbed Mn^{2+} ion, it moves rapidly to other unperturbed Mn^{2+} ions, away from trap 1. What happens to this excitation *after* has no effect on the mean life of trap 1. The evolution of the donor population is affected by the strength of the Mn-Mn coupling as shown by the $RbMn_xMg_{1-x}F_3$ data, not by the presence of the RE acceptors.

*Permanent address: Department of Physics, Boston College, Chestnut Hill, MA 02167.

†Permanent address: Northrop Corporation, Norwood, MA 02062.

‡Permanent address: Avco Everett Research Laboratory, Everett, MA 02149.

[1]R. K. Watts, in *Optical Properties of Ions in Solids*, edited by B. Di Bartolo (Plenum, New York, 1975), p. 307.

[2]R. Greene, D. Sell, R. Feigelson, G. Imbusch, and H. Guggenheim, Phys. Rev. **171**, 600 (1968).
[3]B. A. Wilson, W. M. Yen, J. Hegarty, and G. F. Imbusch, Phys. Rev. B **19**, 4238 (1979); also B. A. Wilson, Ph.D. thesis. University of Wisconsin-Madison, 1978 (unpublished).
[4]K. Gooen, B. Di Bartolo, M. Alam, R. C. Powell, and A. Linz, Phys. Rev. **177**, 615 (1969).
[5]J. Danko, D. Pacheco, and B. Di Bartolo, J. Lumin. **28**, 27 (1983).
[6]A. Mehra and P. Venkateswarlu, J. Chem. Phys. **47**, 2334 (1967).
[7]V. Goldberg, R. Moncorgé, D. Pacheco, and B. Di Bartolo, in *Luminescence of Inorganic Solids*, edited by B. Di Bartolo (Plenum, New York, 1977), p. 603.
[8]J. Danko, D. Pacheco, and B. Di Bartolo, Phys. Rev. B **28**, 2382 (1983).
[9]N. Koumvalakis, W. Sibley, and G. Venikouas, J. Lumin. **15**, 283 (1977).
[10]J. Hegarty, B. A. Wilson, W. M. Yen, T. J. Glynn, and G. F. Imbusch, Phys. Rev. B **18**, 5812 (1978).
[11]J. M. Flaherty and B. Di Bartolo, Phys. Rev. B **8**, 5232 (1973).